



## Communication

Ceria supported Ru<sup>0</sup>-Ru<sup>δ+</sup> clusters as efficient catalyst for arenes hydrogenationYanwei Cao<sup>a,b</sup>, Huan Zheng<sup>a,b</sup>, Gangli Zhu<sup>a,\*</sup>, Haihong Wu<sup>c,\*</sup>, Lin He<sup>a,\*</sup><sup>a</sup> State Key Laboratory for Oxo Synthesis and Selective Oxidation (OSSO), Suzhou Research Institute of LICP, Lanzhou Institute of Chemical Physics (LICP), Chinese Academy of Sciences (CAS), Lanzhou 730000, China<sup>b</sup> University of Chinese Academy of Sciences, Beijing 100049, China<sup>c</sup> Henan Province Key Laboratory of New Opto-Electronic Functional Materials, College of Chemistry and Chemical Engineering, Anyang Normal University, Anyang 455000, China

## ARTICLE INFO

## Article history:

Received 27 April 2020

Received in revised form 15 May 2020

Accepted 30 May 2020

Available online 1 June 2020

## Keywords:

Ceria  
Ruthenium  
Clusters  
Amines  
Hydrogenation

## ABSTRACT

Selective hydrogenation of aromatic amines, especially chemicals such as aniline and bis(4-aminocyclohexyl)methane for non-yellowing polyurethane, is of particular interests due to the extensive applications. To conquer the existing difficulties in selective hydrogenation, the Ru<sup>0</sup>-Ru<sup>δ+</sup>/CeO<sub>2</sub> catalyst with solid frustrated Lewis pairs was developed for aromatic amines hydrogenation with excellent activity and selectivity under relative milder conditions. The morphology, electronic and chemical properties, especially the Ru<sup>0</sup>-Ru<sup>δ+</sup> clusters and reducible ceria were characterized by X-ray diffraction (XRD), transmission electron microscopy (TEM), scanning electronic microscopy (SEM), X-ray photoelectron spectroscopy (XPS), CO<sub>2</sub> temperature programmed desorption (CO<sub>2</sub>-TPD), H<sub>2</sub> temperature programmed reduction (H<sub>2</sub>-TPR), H<sub>2</sub> diffuse reflectance Fourier transform infrared spectroscopy (H<sub>2</sub>-DRIFT), Raman, etc. The 2% Ru/CeO<sub>2</sub> catalyst exhibited good conversion of 95% and selectivity greater than 99% toward cyclohexylamine. The volcano curve describing the activity and Ru state was found. Owing to the "acidic site isolation" by surrounding alkaline sites, condensation between the neighboring amine molecules could be effectively suppressed. The catalyst also showed good stability and applicability for other aromatic amines and heteroarenes containing different functional groups.

© 2020 Chinese Chemical Society and Institute of Materia Medica, Chinese Academy of Medical Sciences. Published by Elsevier B.V. All rights reserved.

Catalytic hydrogenation of aromatic compounds is one of the important organic transformations process in chemical industry [1,2]. The hydrogenated aromatic amines can be exploited in a variety of applications. For instance, cyclohexylamine (CHA), which is produced by hydrogenation of aniline, can be used in the synthesis of dyestuff, plasticizers, emulsifier and rubber vulcanizing additives. Its derivative, bis(4-aminocyclohexyl) methane (H<sub>12</sub>MDA) is an important diamine intermediate for synthesizing various high-value added compounds, like non-yellowing polyurethane. Unfortunately, hydrogenation of aromatic amines usually requires expensive catalysts and harsh conditions. For example, Ru/C catalyst with assistance of alkali additives was applied in the methylenedianline (MDA) hydrogenation reaction under conditions of 18 MPa and 190 °C [3]. Furthermore, under such conditions, it generates many undesirable by-products, which

would deteriorate product quality of polymers, especially in chroma and fiber strength.

To overcome these problems, supported precious metal catalysts have been developed for hydrogenation reactions, such as Ir, Pt, Rh and Ru usually have higher catalytic performance than non-precious metal. Among them, Ru based catalysts have attracted much attention due to their relative low cost (ca. 1/7~1/6 of Pd) and potential excellent catalytic performance by careful modulation of Ru NPs and its interaction between the supports [4,5]. Ceria has been recognized recently as suitable supports in various catalytic processes, owing to its peculiar nature [6], such as surface-bound defects (oxygen vacancy), reducible character, strong interaction between the support and metal. In addition, there are solid frustrated-Lewis-pair sites (FLPs) over ceria [7], which possessed the ability of H—H bond dissociation and expectantly could be advantageous in the hydrogenation reactions [8]. To the best of our knowledge, there are only very limited works reported on hydrogenation of aniline and the derivatives like MDA over Ru/CeO<sub>2</sub> catalysts.

\* Corresponding authors.

E-mail addresses: zhugl@licp.cas.cn (G. Zhu), sailor99600@126.com (H. Wu), helin@licp.cas.cn (L. He).

Herein, the Ru<sup>0</sup>-Ru<sup>δ+</sup>/CeO<sub>2</sub> catalyst with solid frustrated Lewis pairs was developed for aromatic amines hydrogenation with excellent activity and selectivity. The morphology, electronic and chemical properties, especially the Ru<sup>0</sup>-Ru<sup>δ+</sup> clusters and reducible ceria were characterized by X-ray diffraction (XRD), transmission electron microscopy (TEM), scanning electronic microscopy (SEM), X-ray photoelectron spectroscopy (XPS), CO<sub>2</sub> temperature programmed desorption (CO<sub>2</sub>-TPD), H<sub>2</sub> temperature programmed reduction (H<sub>2</sub>-TPR), H<sub>2</sub> diffuse reflectance Fourier transform infrared spectroscopy (H<sub>2</sub>-DRIFT), Raman spectroscopy, etc. The volcano curve describing the activity and Ru loading amount was found. And the "acidic site isolation" by surrounding alkaline sites effect was proposed for the high selectivity.

The experimental section, including chemicals, catalysts preparation (synthesis of Ru/CeO<sub>2</sub>), characterization, catalytic hydrogenation experiments can be found in Supporting information

The XRD patterns were given in Fig. 1. As shown, the characteristic diffraction peaks with 2θ at 28.5°, 33.1°, 47.5°, 56.3°, 59.1°, 69.4° and 76.7°, which can be indexed to the (111), (200), (220), (311), (222), (400) and (331) planes of face-centered cubic phase ceria (space group Fm-3m, ref. 01-081-0972), appeared in the patterns. However, the peaks for Ru species were not observed even the loading amount reached 4%. This may be caused by small size of Ru clusters, disordered lattice structure, and high dispersion of Ru species due to an interaction with ceria support [9].

Pyridine adsorption IR patterns (Fig. 1b) showed Lewis acidic nature of ceria surface, indicated by IR bands at 1441, 1570 and 1592 cm<sup>-1</sup> appearance [10]. CO<sub>2</sub>-TPD showed the alkaline nature of ceria surface (Fig. 1c) and the strength of the base was enhanced after Ru loading. The coexistence of acidic and alkaline sites can be explained by solid frustrated-Lewis-pair sites on ceria surface [7].

SEM, HAADF-TEM microscopy and EDX spectroscopy were used to study the morphologies and elemental distribution of Ru/CeO<sub>2</sub> catalyst. As shown in Fig. 2, the catalyst was comprised of nanoparticles staking together, and the elemental mapping showed that Ce, O and Ru species were in good dispersion throughout the catalyst, possibly due to interfacial anchoring by immobilization effect of surface oxygen vacancies [10]. Ru clusters mainly deposited on the (111) surface of ceria. Some Ru clusters with diameter of 2~3 nm could be observed, exposing their hcp (101) planes with lattice spacing of 0.21 nm. Ru loading amount would influence the size of Ru clusters. 4% Ru loading leading to formation of relative large nanoparticles (ca. 5~8 nm) and there were hardly countable Ru nanoparticles were found in 0.5% Ru/CeO<sub>2</sub> and 1% Ru/CeO<sub>2</sub> TEM images (Fig. S4 in Supporting information). Some crystal plane structures of the Ru clusters were disordered (Fig. 2c), indicating part of Ru clusters were oxidized to form disordered Ru<sup>δ+</sup> layers due to interfacial Ru-O-Ce anchoring. Some oxygen in ceria with high mobility may also

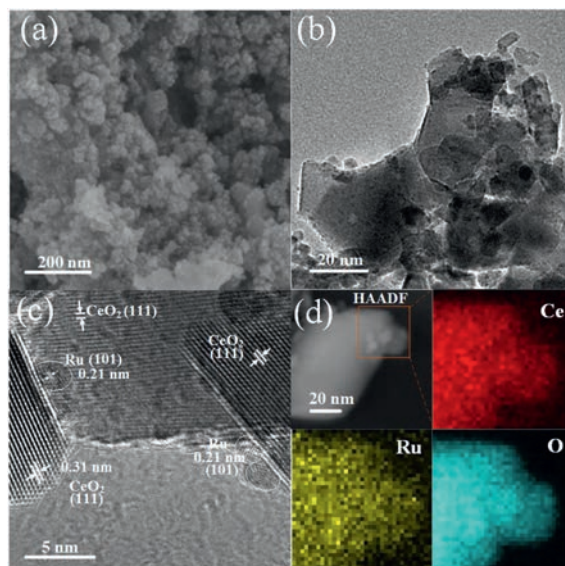


Fig. 2. Morphological and elemental analysis of 2%Ru/CeO<sub>2</sub>: (a) SEM image; (b) TEM image; (c) HRTEM image; (d) elemental mapping.

transfer to Ru clusters, while simultaneously, ceria layers at the perimeter of the particles would be reduced, [11,12] which turned out to be an interaction effect. The chemical nature change of Ru clusters, oxidation of the Ru clusters accompanying reduction of Ce<sup>4+</sup> to Ce<sup>3+</sup> cations, would consequently influence the activity as it will be showed in the catalytic performance results.

The interaction strength can be reflected in the reducibility. H<sub>2</sub>-TPR was performed and the results are shown in Fig. 3a. There are two peak regions in the TPR profiles, with region I at low temperatures and region II at high temperatures, attributed to the reduction of Ru species with different interaction strength with support [10,13]. In the 2% Ru/SiO<sub>2</sub>, the reduction peaks at 133 °C and 246 °C for both two regions were higher than 2% Ru/CeO<sub>2</sub>. The reducibility was not only affected by support types but also the Ru loading amount. In the ceria supported catalysts, region I could be ascribed to reduction of partially oxidized Ru particles that had weak interaction with support. This peak region I shift from 160 °C to 105 °C when the Ru loading amount increased from 1% to 2%. Further raising Ru amount to 4% did not result a lower reduction temperature but led to region I splitting into 3 consecutive peaks, corresponding to the stepwise reduction of supported ruthenium oxides. With regards to the 2% Ru/CeO<sub>2</sub>, the region I initiated from 55 °C and ended at 172 °C. The high reducibility indicated the interaction between Ru clusters and ceria was relative weak with this loading amount, which was also verified by Raman character-

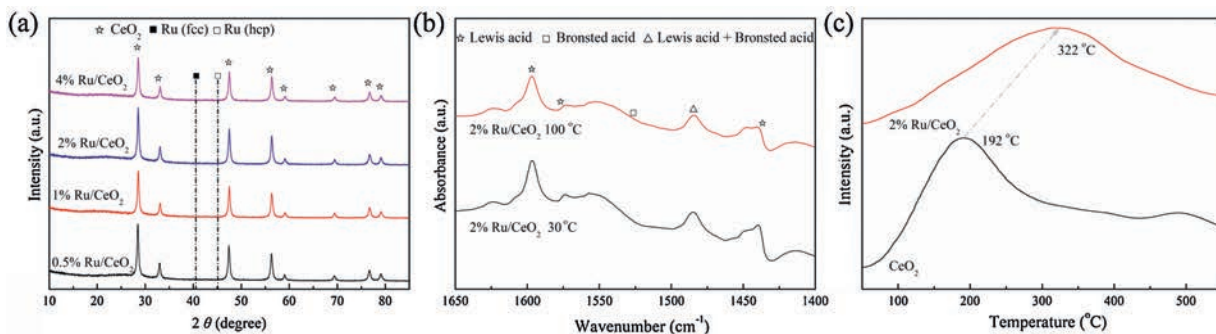


Fig. 1. (a) XRD patterns for different Ru-based catalysts. (b) Pyridine adsorption IR of Ru/CeO<sub>2</sub> catalysts. (c) CO<sub>2</sub>-TPD curves of 2% Ru/CeO<sub>2</sub> catalyst and CeO<sub>2</sub> support.

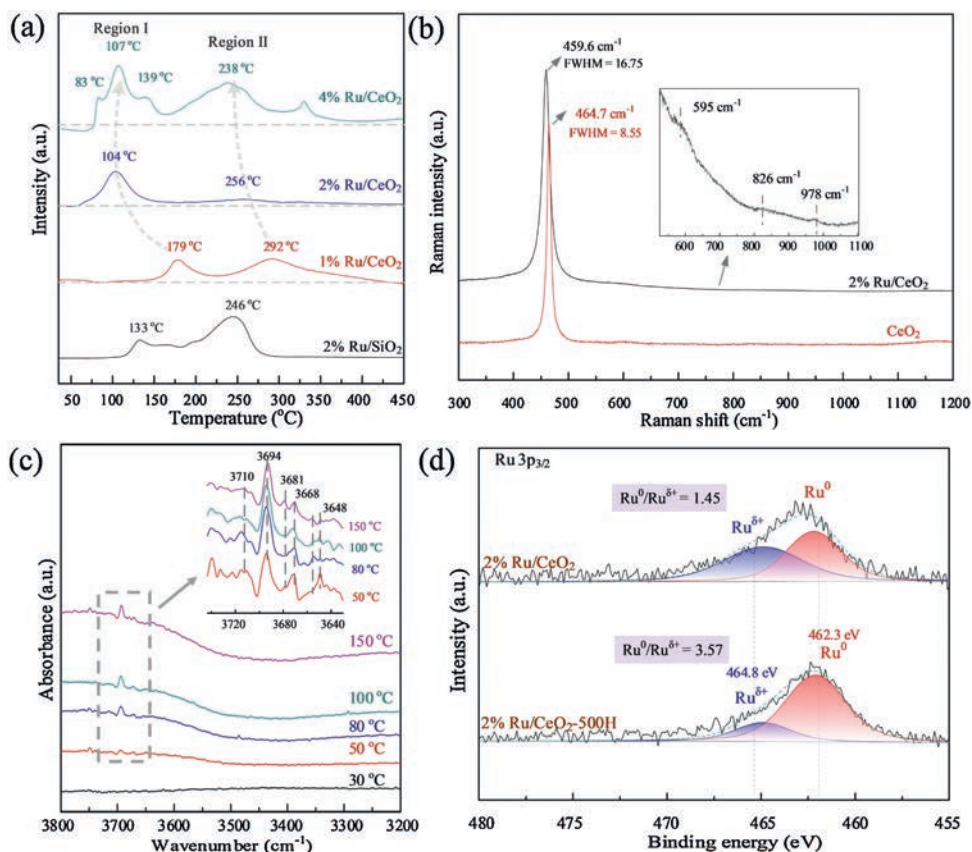


Fig. 3. Supported Ru catalysts (a)  $\text{H}_2$ -TPR profiles, (b) *in-situ*  $\text{H}_2$ -DRIFTS spectra, (c) Raman spectra and (d) XPS spectra of Ru  $3p_{3/2}$ .

The Raman spectroscopy (Fig. 3b) showed that there was a peak at  $978\text{ cm}^{-1}$ , which can be attributed to Ru–O–Ce [10,14], but the intensity was quite weak due to the relative low defects density of stable (111) planes of ceria [15]. The broad TPR peak region II at high temperature can be attributed to the reduction of Ru species which strongly interact with ceria. The reduction peak shifted to lower temperature with increase of Ru content. This peak decreased from  $292\text{ }^\circ\text{C}$  to  $238\text{ }^\circ\text{C}$  when the Ru amount increased from 1% to 4%. These Ru species were oxidized to a greater extent by the higher affinity of oxygen which was provided by supports (*i.e.*, higher absorption enthalpy of oxygen) [16]. And thus, these Ru species, which strongly interact with support, are relatively not easy to be reduced.

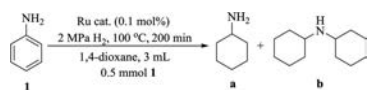
In the reduction process, the spill-over of hydrogen from the metal to the support could be observed by the  $\text{H}_2$ -DRIFT (Fig. 3c). Hydrogen may be adsorbed on surface oxygen after dissociation, resulting to formation of –OH groups. Comparing with the curve of sample pretreated at  $200\text{ }^\circ\text{C}$  in vacuum, after  $\text{H}_2$  injection, new absorption bands at range of  $3620\text{--}3720\text{ cm}^{-1}$  appeared since  $50\text{ }^\circ\text{C}$ , which are attributable to –OH species [17,18]. Especially, bands at  $3681\text{ cm}^{-1}$  was supposed as doubly bridging OH species (denoted as OH(II\*-A)) when ceria surface was exposed to  $\text{H}_2$  and bands at  $3648\text{ cm}^{-1}$  was supposed to be doubly bridging OH species related to abundant oxygen vacancy (denoted as OH(II\*-B)) [18]. These results illustrated that Ru species could be partially reduced at low temperatures and spill-over of hydrogen from Ru clusters to support could take place after  $\text{H}_2$  dissociation. The hydroxylation of oxide surfaces driven by molecular  $\text{H}_2$  dissociation could play an important role in redox reactions [19]. In this work, the reaction temperature was  $100\text{--}150\text{ }^\circ\text{C}$ , which was higher than the initial activation temperature, the hydrogenation reaction

could benefit greatly from the  $\text{H}_2$  readily dissociation and transferring by spilling-over.

The chemical state of the supported Ru catalysts was investigated by XPS. As indicated in Ru  $3p_{3/2}$  signal (Fig. 3d and Fig. S5 in Supporting information), the peak at bind energy (BE)  $462.2\text{ eV}$  can be attributed to  $\text{Ru}^0$ , while the peak at higher BE can be assigned to positively charged Ru (BE  $464.8\text{ eV}$ ) [13,20]. As shown, the electronic state of Ru can be readily tuned by changing Ru loading amount. The relative atomic ratio of  $\text{Ru}^0/\text{Ru}^{\delta+}$  was quantified by fitted Ru  $3p$  peaks. As found, the  $\text{Ru}^0/\text{Ru}^{\delta+}$  ratio increased from 0.23 to 1.45 when the Ru amount increased from 0.5% to 2%. The ratio only slightly increased to 1.47 while further double Ru amount to 4%. Because the electronic state of Ru variation reflects the chemical interfacial Ru–O–Ce bonding interaction between Ru clusters and ceria support [13], the  $\text{Ru}^0/\text{Ru}^{\delta+}$  ratio variation trend suggested that the electronic interaction was weakened by increasing Ru loading amount from 0.5% to 2%. Since  $\text{Ru}^0/\text{Ru}^{\delta+}$  ratio could not be significantly raised when the Ru loading amount was higher than 2%, to investigate the case of high  $\text{Ru}^0/\text{Ru}^{\delta+}$  ratio, we deliberately reduced the sample of 2% Ru/CeO<sub>2</sub> at  $500\text{ }^\circ\text{C}$  in  $\text{H}_2$  atmosphere. As seen in Fig. 4, the  $\text{Ru}^0/\text{Ru}^{\delta+}$  ratio was raised to 3.57. However, Ru species were still not completely reduced due to the interaction between Ru clusters and ceria. The XPS spectra of Ce 3d and O 1s were well analyzed (Fig. S6 in Supporting information).

Hydrogenation of aniline was carried out with prepared catalysts (Table 1). As shown, the 2% Ru/CeO<sub>2</sub> catalysts had a good catalytic performance, providing as high as conversion of 95% and selectivity of 99% toward cyclohexylamine (entry 3). The side-products by hydrodealkylation or condensation reaction (*e.g.*, dicyclohexylamine) were not observed in the reaction. Comparing

**Table 1**  
Hydrogenation performance using various catalysts.



Entry	Catalyst	Con. (%) <sup>a</sup>	Sel. (%) <sup>b</sup>	
			a	b
1	0.5% Ru/CeO <sub>2</sub>	18	>99.9	–
2	1% Ru/CeO <sub>2</sub>	37	>99.9	–
3	2% Ru/CeO <sub>2</sub>	95	>99.9	–
4	4% Ru/CeO <sub>2</sub>	66	>99.9	–
5	2% Ru/Al <sub>2</sub> O <sub>3</sub>	70	99	1
6	2% Ru/SiO <sub>2</sub>	56	98	2
7	2% Ru/TiO <sub>2</sub>	33	99	1
8	2% Ru/MCF	44	95	5
9 <sup>b</sup>	Ru/C	56	60	40
10 <sup>c</sup>	2% Ru/CeO <sub>2</sub> -500H	28	>99.9	–
11 <sup>d</sup>	2% Ru/CeO <sub>2</sub> -3000	0	–	–

<sup>a</sup> Conversion and selectivity were determined by GC, biphenyl as calibrated internal standard.

<sup>b</sup> Commercial Ru/C catalyst purchased from Aladdin.

<sup>c</sup> 2% Ru/CeO<sub>2</sub> catalyst pretreated at 500 °C in H<sub>2</sub> atmosphere.

<sup>d</sup> 2% Ru/CeO<sub>2</sub> catalyst pretreated at 300 °C in air.

with oxide support or commercial activated carbon, the ceria showed better both activity and selectivity. The catalyst was also effective for MDA hydrogenation process. As shown in Table S1 (Supporting information), comparing with the existing catalysts (or catalyst systems), the 2% Ru/CeO<sub>2</sub> catalyst in this work exhibited quite high catalytic efficiency and selectivity under milder conditions. The catalyst also showed good stability and applicability of other aromatic compound with different functional groups (Figs. S7 and S8 in Supporting information).

In addition, the effect of Ru loading amount was investigated. To be comparable, the same Ru content was used in each reaction entry (Ru 0.1 mol% of substance). Interestingly, the activity did not increase monotonically with Ru loading amount and showed the volcano curve with the optimal activity at 2% Ru, indicating that the interaction between Ru and ceria was not the stronger the better. Take 0.5% Ru/CeO<sub>2</sub> for example, when the Ru clusters have strong interaction with ceria, they were highly oxidized (with Ru<sup>0</sup>/Ru<sup>δ+</sup> ratio of 0.23), as showed by the XPS results. The activity was only less than 1/5 that of 2% Ru/CeO<sub>2</sub>. On the other side, when the ratio of Ru<sup>0</sup>/Ru<sup>δ+</sup> was raised to 1.47 (4% Ru/CeO<sub>2</sub>), the activity showed no further increase but slight decline. To clearly show the influence of Ru<sup>0</sup>/Ru<sup>δ+</sup> ratio, 2% Ru/CeO<sub>2</sub> was deliberately reduced at temperature as high as 500 °C in H<sub>2</sub> atmosphere. The Ru<sup>0</sup>/Ru<sup>δ+</sup> ratio was as high as 3.57 and the conversion dropped to only 28%. Finally, it goes without saying that the particle size of Ru nanoparticles was another key reason for the catalytic performance.

The high catalytic performance originated from the unique properties of ceria support and the suitable interaction with Ru clusters. When the Ru clusters anchored with ceria support by Ru—O—Ce, part of them was oxidized to Ru<sup>δ+</sup>, meanwhile, parts of Ce<sup>4+</sup> cations were reduced to Ce<sup>3+</sup> with acidic nature and some oxygen vacancies were also created. Ru<sup>0</sup>-Ru<sup>δ+</sup> clusters over ceria surface with FLPs could facilitate H<sub>2</sub> heterolytic dissociation at low temperatures and Lewis acids can activate aromatic compounds [8,21–23]. When the interaction between Ru clusters and ceria was too strong, Ru clusters may be oxidized to a high degree. The reduction of Ru and H<sub>2</sub> dissociation was not likely to occur. Conversely when the interaction was too weak, Ru particles would start to grow up and the dispersion of Ru particles became worse due to shortage of bonding anchoring. More importantly, spilling-

over and storage of H in the form of —OH may be not sufficient to a certain degree due to lacking intimate interfacial interaction by Ru—O—Ce bonding. density functional theory (DFT) calculations also demonstrated that oxygen vacancies were in favor of the stabilization of hydridic H species in ceria [24]. Both the high metal dispersion, Lewis acid sites and the abundance of H species by H<sub>2</sub> dissociation could enhance the hydrogenation of aniline.

The high selectivity and low condensation side-products can be explained by to the coexistence of solid frustrated Lewis acid-base pair sites over ceria [7]. For a general acidic support, aniline and cyclohexylamine molecules have strong adsorption on acidic sites [25,26]. And condensation reaction may take place between the neighboring molecules. However, regarding with ceria, which has a fluorite-like cubic structure. Each cerium atom possessing the Lewis acid nature is surrounded by the surface and subsurface alkaline oxygen sites (and even enhanced by oxygen vacancies). This "acidic site isolation" of Lewis acid sites by alkaline sites could effectively suppress condensation of amines. Similar results also observed in selective hydrogenation of alkynes [17], a low degree of oligomerization of intermediates was found in the conversion of alkynes to olefins over CeO<sub>2</sub>.

In summary, the well-tuned Ru/CeO<sub>2</sub> was demonstrated as efficient catalyst for aromatic amines hydrogenation with excellent activity and selectivity. Morphology, electronic and chemical properties of Ru/CeO<sub>2</sub> was well were analyzed by using different characterization techniques. Due to the special chemical nature of Ru/CeO<sub>2</sub>, the catalyst exhibited good conversion of 95% and selectivity of 99.9% toward cyclohexylamine. The catalyst also showed superior stability and applicability of other aromatic amines and heteroarenes containing different functional groups.

## Declaration of competing interest

The authors declare that they have no known competing financial interests or personal relationships that could have appeared to influence the work reported in this paper.

## Acknowledgments

This research was financially supported by the Youth Innovation Promotion Association CAS (No. 2018453) and the National Natural Science Foundation of China (No. 91645118 for L. He, 21773270 for G. Zhu). Supports from the NSF of Jiangsu Province (No. BK20180249) are also gratefully acknowledged.

## Appendix A. Supplementary data

Supplementary material related to this article can be found, in the online version, at doi:<https://doi.org/10.1016/j.ccl.2020.05.045>.

## References

- [1] Z. Wei, Y. Li, J. Wang, et al., *Chin. Chem. Lett.* 29 (2018) 815–818.
- [2] Z.Q. Liu, X.Y. Wei, F.J. Liu, et al., *Fuel* 223 (2018) 222–229.
- [3] W. Hayazaki, H. Omori, K. Ozaki, JP2002348267A, 2002.
- [4] G.Y. Fan, W.J. Huang, *Chin. Chem. Lett.* 25 (2014) 359–363.
- [5] H.Z. Bi, R.F. Dou, H. Wang, et al., *Acta Phys.-Chim. Sin.* 32 (2016) 1765–1774.
- [6] T. Montini, M. Melchionna, M. Monai, et al., *Chem. Rev.* 116 (2016) 5987–6041.
- [7] S. Zhang, Z.Q. Huang, Y. Ma, et al., *Nat. Commun.* 8 (2017) 15266.
- [8] M. Garcia-Melchor, N.R. Lopez, *J. Phys. Chem. C* 118 (2014) 10921–10926.
- [9] B. Ouyang, W. Tan, B. Liu, *Catal. Commun.* 95 (2017) 36–39.
- [10] J. An, Y. Wang, J. Lu, et al., *J. Am. Chem. Soc.* 140 (2018) 4172–4181.
- [11] N. Ta, J. Liu, S. Chenna, et al., *J. Am. Chem. Soc.* 134 (2012) 20585–20588.
- [12] A. Figueroba, G. Kovacs, A. Bruix, et al., *Catal. Sci. Technol.* 6 (2016) 6806–6813.
- [13] Y. Guo, S. Mei, K. Yuan, et al., *ACS Catal.* 8 (2018) 6203–6215.
- [14] F. Wang, C.M. Li, X.Y. Zhang, et al., *J. Catal.* 329 (2015) 177–186.
- [15] Z.A. Qiao, Z. Wu, S. Dai, *ChemSusChem* 6 (2013) 1821–1833.
- [16] P.G.J. Koopman, A.P.G. Kieboom, H. Van Bekkum, *J. Catal.* 69 (1981) 172–179.
- [17] G. Vilé, B. Bridier, J. Wichert, et al., *Angew. Chem., Int. Ed.* 51 (2012) 8620–8623.

- [18] Z. Mo, Y. Sun, H. Chen, et al., *Polymer* 46 (2005) 12670–12676.
- [19] F.R. Negreiros, M.F. Camellone, S. Fabris, *J. Phys. Chem. C* 119 (2015) 21567–21573.
- [20] A. Arico, P. Creti, H. Kim, et al., *J. Electrochem. Soc.* 143 (1996) 3950–3959.
- [21] Z.Q. Huang, L.P. Liu, S. Qi, et al., *ACS Catal.* 8 (2018) 546–554.
- [22] A.M. Rasero-Almansa, A. Corma, M. Iglesias, et al., *Green Chem.* 16 (2014) 3522–3527.
- [23] S. Zhang, M. Zhang, Y. Qu, *Acta Phys.-Chim. Sin.* 36 (2020) 1911050.
- [24] K. Werner, X. Weng, F. Calaza, et al., *J. Am. Chem. Soc.* 139 (2017) 17608–17616.
- [25] W. Liang, M. Cui, J. Tang, et al., *J. Nanjing Tech Univ. (Nat. Sci. Ed.)* 02 (2014) 89–94.
- [26] F. Chen, C. Topf, J. Radnik, et al., *J. Am. Chem. Soc.* 138 (2016) 8781–8788.